ADVANCED NANOBIOMED RESEARCH
www.advnanobiomedres.com

Comparative Antimicrobial Properties of Sodium Borate and Carbonate and their Perborate and Percarbonate Counterparts

*Ayden Watt, Dario Job, Justin Matta, Nitin Chandra Teja Dadi, Cat-Thy Dang, Yara Raphael, Joshua Vorstenbosch, Geraldine Merle, and Jake Barralet**

Antimicrobial resistance (AMR) poses a significant challenge in wound management, particularly in ischemic and chronic wounds, which are prone to infection and where traditional treatments often fall short. In response to this need, the antibacterial activity of polycaprolactone (PCL) films, composited with sodium perborate and sodium percarbonate to provide controlled release of oxygen and reactive oxygen species, is compared in vitro and in vivo. Sustained antimicrobial action against both Gram-positive and Gram-negative bacteria is measured in vitro that allowed lower quantities to be used compared with the borate and carbonate counterparts sodium borate and carbonate. This effect is also observed in vivo, such that perborate formulations are effective at wound treatment using one-tenth the borate concentration required in sodium borate formulations. Overall, sodium perborate-loaded films significantly accelerate wound closure, reduce bacterial load, and enhance early-phase wound healing, outperforming borate equivalent counterparts at equivalent loading levels. In addition to effectively inhibiting bacterial growth, these composites prevent biofilm formation in vitro. These findings suggest that perborate-loaded polymeric films could be a powerful tool in advanced wound care, offering both potent antimicrobial effects and promotion of wound healing in complex clinical settings.

1. Introduction

Antimicrobial resistance (AMR) is denoted by the World Health Organization as one of the top global public health and development threats, with 4.95 million antibiotic resistance-associated deaths in 2019.[1] Antimicrobial drugs are classified by their mechanism of action, namely one or more of the following: inhibition of cell wall synthesis, cell membrane depolarization, protein synthesis inhibition, nucleic acid synthesis inhibition, and metabolic inhibition.[2] Despite the broad range of targets for antimicrobial activity, bacteria are capable at adapting to survival following exposure to these chemicals.[2]

Consequently, the search for antibiotic adjuncts is an active field of research that aims to use currently available drugs augment antibiotic efficacy based on their primary mechanism of action.[3–5] However, these strategies are predominantly intended for systemic treatment of bacterial infection and are less applicable for the topical treatment of wounds. Local wound ischemia decreases the bioavailability of delivered drugs, and so antimicrobial wound dressings and materials-based approaches to managing infection have become a critical research direction.[6,7] Further, antimicrobial approaches offer an opportunity to target a broad spectrum of bacteria while minimizing the risk of developing resistance. The use of hydrogen peroxide as a topical antiseptic has led to increased interest in materials-based approaches that sustain reactive oxygen species (ROS) delivery as a primary antimicrobial mechanism.[8,9] Solid

A. Watt, J. Matta, N. C. T. Dadi, J. Vorstenbosch, J. Barralet
Division of Surgical and Interventional Sciences
Department of Surgery
Faculty of Medicine and Health Sciences
Montreal General Hospital
Montreal, QC H3G 1A4, Canada
E-mail: jake.barralet@mcgill.ca

The ORCID identification number(s) for the author(s) of this article can be found under https://doi.org/10.1002/anbr.202500045.

D. Job, C.-T. Dang, Y. Raphael, G. Merle
Chemical Engineering
Polytechnique Montréal
Montreal H3T 1J4, Canada

J. Vorstenbosch
Division of Plastic and Reconstructive Surgery
McGill University Health Centre
Montreal H3G 1A4, Canada

J. Barralet
Faculty of Dental Medicine and Oral Health Sciences
McGill University
2001 McGill College Avenue, Montreal, QC H3A 1G1, Canada

© 2025 The Author(s). Advanced NanoBiomed Research published by Wiley-VCH GmbH. This is an open access article under the terms of the Creative Commons Attribution License, which permits use, distribution and reproduction in any medium, provided the original work is properly cited.

DOI: 10.1002/anbr.202500045

peroxide materials, such as calcium peroxide (CaO_2) and magnesium peroxide (MgO_2), generate ROS upon exposure to wound moisture, producing hydrogen peroxide (H_2O_2), superoxide (O_2^-), and hydroxyl radicals (•OH). These ROS disrupt bacterial cell walls, internal cellular components, and DNA replication.[10–12] Previously, work by our group demonstrated the in vitro antimicrobial activity of several metal peroxides in a PCL film system and there have been several reports showing efficacy in infected wound models.[13–17]

Sodium carbonate (Na_2CO_3) and sodium borate ($Na_2B_4O_7$) have a long history of use as disinfecting agents and cleaners. Sodium carbonate is considerably alkaline and as such is considered unsuitable for direct use on wounds. There are claims of beneficial effects of borates on wound healing; however, there are also health issues surrounding their use. In particular, the European Chemicals Agency recognized that high levels of exposure to borax may adversely affect human reproduction or development, and it is not recommended for use on broken skin by some agencies.[18,19]

However, as attributed to Paracelsus, "dose makes the poison" and the perborate and percarbonate counterparts of these compounds offer the additional effect of ROS and oxygen release.[20–22] We then sought to determine if the perborate and percarbonate forms of these salts could allow for a lower loading level to attain a given antibacterial and wound healing effect.

In this work, we compare the antimicrobial activity of these salts composited with PCL. The film system decreases mammalian cell toxicity by including a catalyst to prevent excessive hydrogen peroxide formation and an acidic salt to mitigate pH elevation and fluctuation as reported previously.[13,23,24] Antimicrobial activity against *S. aureus* and *P. aeruginosa*, two bacteria that commonly cause hospital infections and are known for their potential to develop resistance, was measured in vitro through antibacterial and biofilm formation assays. The physical, chemical, mechanical and cytotoxicity properties of these films were evaluated. The in vivo impact of films made with these antibacterial materials on wound healing was evaluated in a rat ischemic dorsal flap full thickness wound model, alongside their effect on bacterial colonization.

2. Results

2.1. Physicochemical Characterization of Composite Films

The physicochemical properties were evaluated of polymeric films containing sodium perborate (SPB)/sodium percarbonate (SPC), which are highly reactive and decompose to form carbonate and borate salts in water. Films were batch prepared with 20, 200, and 2000 mg of SPC or SPB, corresponding to relative concentrations of 0.15%, 1.5%, and 13.4 wt% (**Figure 1**). For in vitro assays, small 6 mm disks were cut from the batch preparation with corresponding SPB/SPC loading levels of 0.02 mg, 0.2 mg, and 2 mg respectively. For in vivo experiments, 2 × 3 cm rectangular films were used. The swelling index (S.I) for all samples was stable over time and increased with increasing loading level (Figure S1A, Supporting Information). Films in the 20 and 200 mg groups had similar SI values to the control, while higher loading levels (2000 mg) had significantly higher SI values of around 6–9%. All samples had Young's moduli of between 300 and 400 MPa (Figure S1B, Supporting Information). The SPB2000 had the highest modulus, which was significantly higher than the SPC groups ($P < 0.05$).

2.2. Composite Film Degradation and Release

The oxygen release (**Figure 2**A,B) of the film formulations indicated that, as expected, higher loading levels of SPC and SPB led to greater oxygen release. All samples in the 200 mg group or less of percarbonate/perborate released very little oxygen. The controlled release of oxygen and hydrogen peroxide from SPC- and SPB-loaded PCL films is critical for determining both antimicrobial efficacy and cellular cytotoxicity. At the highest loading levels (SPB2000 and SPC2000), the films released significant oxygen, with SPB2000 reaching peak levels of 571 µM, nearly double that of SPC2000. Similarly, hydrogen peroxide release was higher for SPB than SPC, with SPB2000 sustaining concentrations up to 600 µM (Figure 2C,D) sufficient to inhibit bacterial growth. The greater solubility of SPB compared to SPC likely contributed to these differences.

Figure 2E–H shows that pH increased over time in each sample and that the final pH depended on the total loading

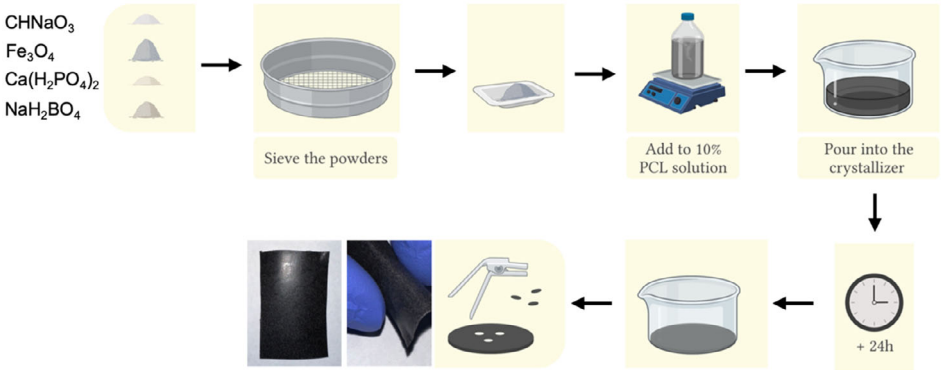

Figure 1. Sample production steps. All components are sieved, added to a PCL-chloroform solution and poured into a crystallizer. After 24 h drying, circular pieces 6 mm in diameter or flexible rectangular sheets 3 × 4 cm were cut for experiments.

© 2025 The Author(s). Advanced NanoBiomed Research published by Wiley-VCH GmbH

26999307, 2025, 8, Downloaded from https://advanced.onlinelibrary.wiley.com/doi/10.1002/anbr.202500045 by Polytechnique Montreal, Wiley Online Library on [09/03/2026]. See the Terms and Conditions (https://onlinelibrary.wiley.com/terms-and-conditions) on Wiley Online Library for rules of use; OA articles are governed by the applicable Creative Commons License

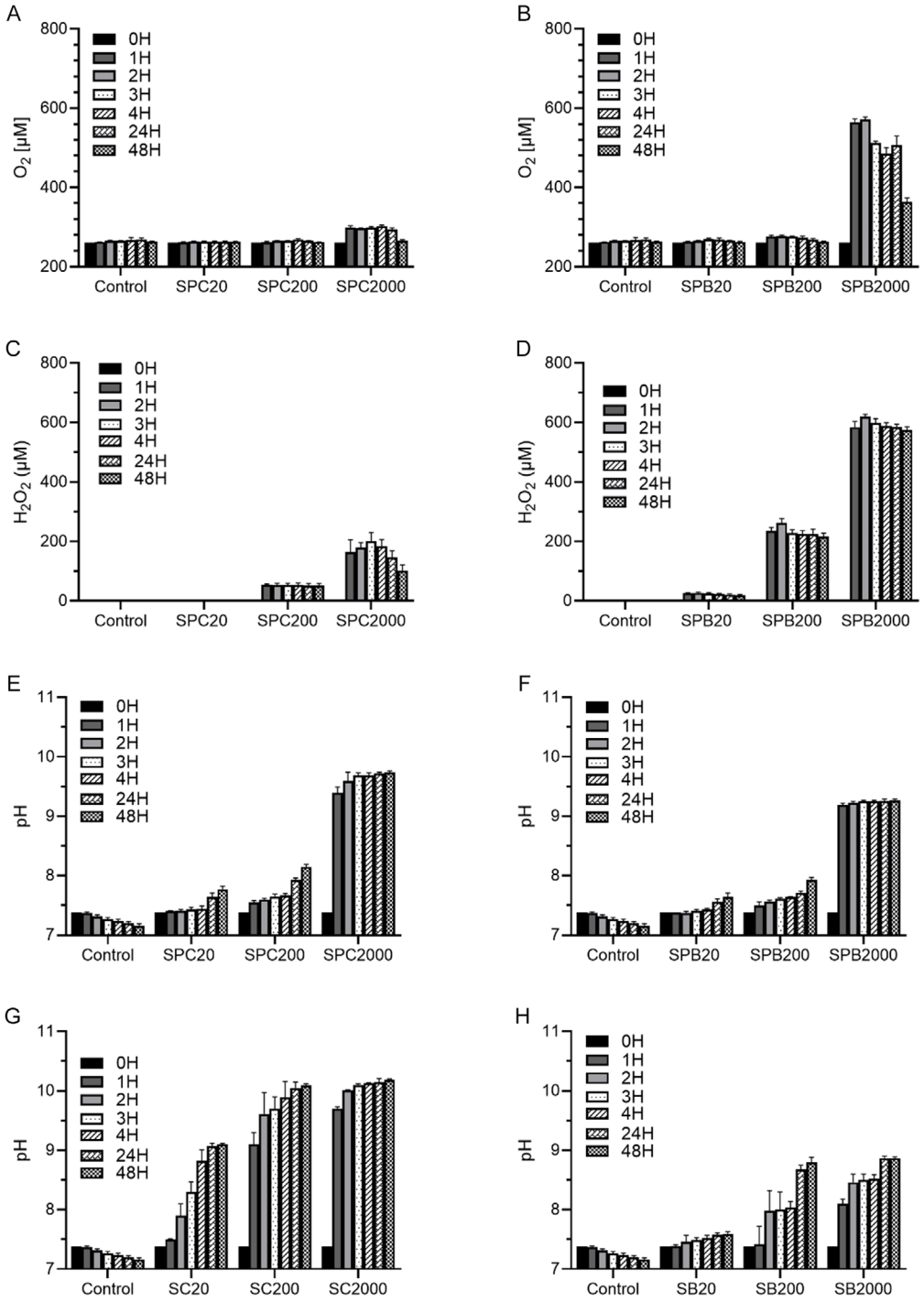

Figure 2. Material characterization of loaded PCL films. A,B) Oxygen concentration, C,D) Hydrogen peroxide release, E–H) pH of solutions containing samples measured up to 48 h (mean ± SD; $N = 3$).

level. The pH increased gradually for the 20 and 200 mg groups, with peak values of 7.8 and 7.6 for SPC20 and SPB20 respectively, and 8.2 and 7.9 for SPC200 and SPB200. The two 2000 mg samples raised pH considerably to 9.7 and 9.3 for SPC2000 and SPB2000 respectively. pH levels of solutions in which SB films were stored were broadly comparable to SPB films, but slightly lower (≈0.5 pH points). SC films raised pH levels ≈0.5 pH points higher than SPC films, reaching 9.1, 10.1, and 10.2 for SC20, SC200, and SC2000 respectively.

© 2025 The Author(s). Advanced NanoBiomed Research published by Wiley-VCH GmbH

26999307, 2025, 8, Downloaded from https://advanced.onlinelibrary.wiley.com/doi/10.1002/anbr.202500045 by Polytechnique Montreal, Wiley Online Library on [09/03/2026]. See the Terms and Conditions (https://onlinelibrary.wiley.com/terms-and-conditions) on Wiley Online Library for rules of use; OA articles are governed by the applicable Creative Commons License

2.3. Antibacterial Activity

The antimicrobial activity of the carbonate, percarbonate, borate and perborate samples against *S. aureus*, a Gram-positive bacterium, and *P. aeruginosa*, a Gram-negative bacterium, were compared in vitro and their capacity to inhibit biofilm formation was assessed (**Figure 3**). SPC or SPB films in the 200 or 2000 mg groups had significant and prolonged antibacterial effect for over the three days for both bacterial strains (Figure 3A–D). In 2000 mg groups, after 48–72 h (Figure 3A–D), bacterial counts were six orders of magnitude lower. SPB appeared to have the greatest antibacterial activity since films in the 200 mg group also effectively eliminated bacteria. SC and SB had little to no effect on reducing bacterial counts.

Biofilm inhibition was observed only in SPB2000, where H_2O_2 concentrations exceeded 600 µM. This suggests that while ROS contribute to bacterial inhibition, their sustained presence is necessary to prevent biofilm formation.

2.4. In Vitro Cytotoxicity

Human dermal fibroblast (HDF) viability was evaluated after 24, 48, and 72 h of incubation with films (**Figure 4**). Generally percarbonates seem less cytotoxic than their carbonate counterparts and the reverse was observed for borates and perborates. Fibroblast viability was unaffected by SPC20 and 200 but dropped drastically to ≈30% on day 1% and 15% on day 3 when exposed to SPC2000. Viability for SPB200 was around 40% over the duration of the experiment and below 10% for SPB2000. SC progressively resulted in a decrease in cell viability as loading level increased, with the lowest fibroblast survival being roughly 30% at 24 h and 10% at 72 h with SC2000. SB appeared less cytotoxic, with even the SB2000 condition maintaining 60% viability rate over 72 h.

2.5. In Vivo Ischemic Wound Healing

In light of the higher antibacterial activity of borates and perborates than carbonates and percarbonates (Figure 3), the effects of sodium borate and SPB delivery to wounds in vivo were subsequently compared.

The antibacterial effects of borate and perborate films were investigated in an in vivo ischemic rat wound model. Bacterial culture swabs were collected from 8 mm full thickness wounds every 2 days postoperatively until day 10 (**Figure 5**A). All wounds

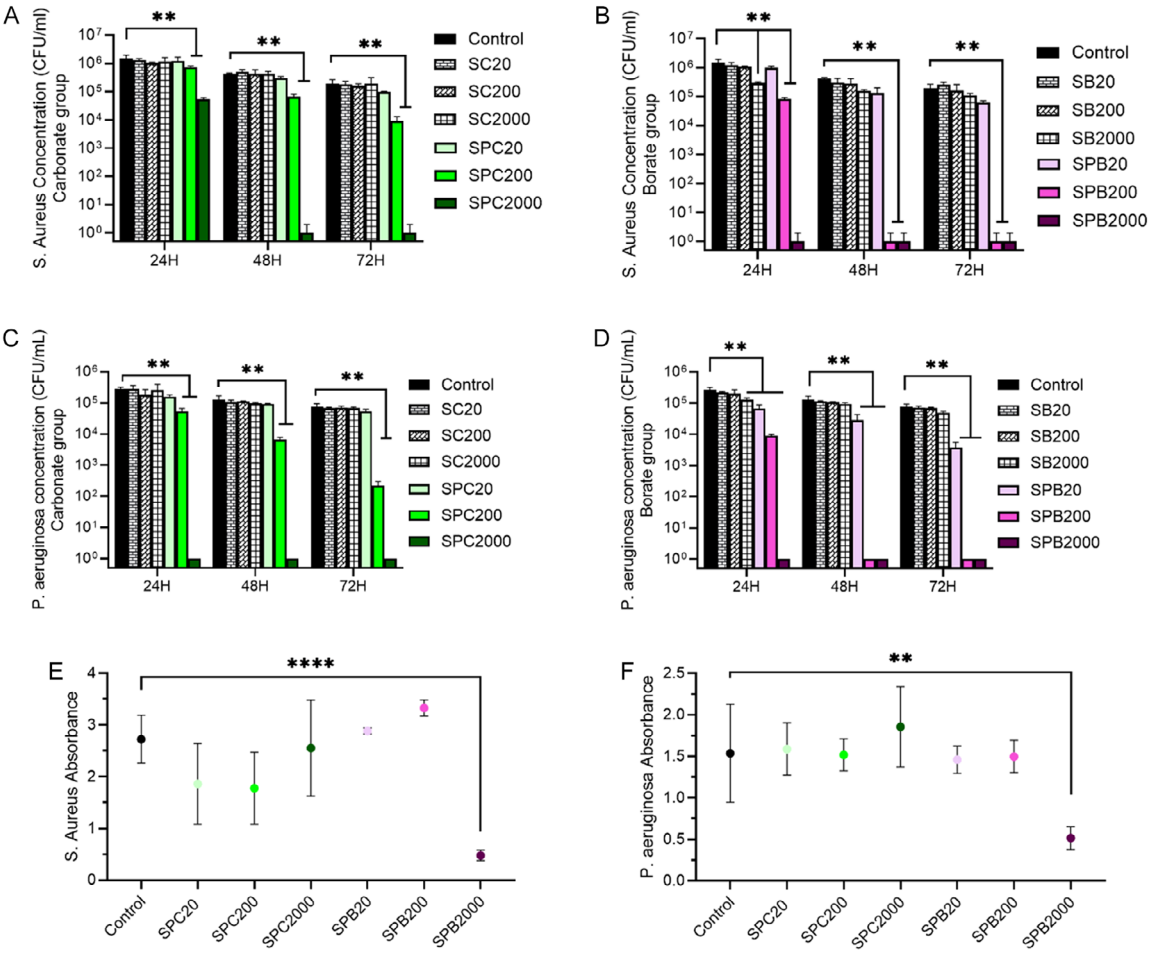

Figure 3. A,B) Calculated bacterial concentration for *S. aureus* C,D) and *P. aeruginosa* with plate count assays up to 72 h (mean ± SD; $N = 3$). E) In vitro biofilm formation with *S. aureus* F) and with *P. aeruginosa* (mean ± SD; $N = 9$, $^{**}P < 0.01$, $^{****}P < 0.0001$).

© 2025 The Author(s). Advanced NanoBiomed Research published by Wiley-VCH GmbH

26999307, 2025, 8, Downloaded from https://advanced.onlinelibrary.wiley.com/doi/10.1002/anbr.202500045 by Polytechnique Montreal, Wiley Online Library on [09/03/2026]. See the Terms and Conditions (https://onlinelibrary.wiley.com/terms-and-conditions) on Wiley Online Library for rules of use; OA articles are governed by the applicable Creative Commons License

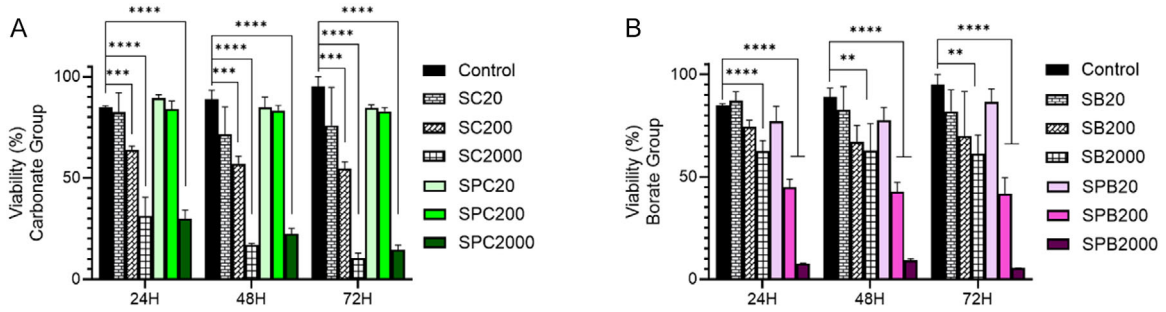

Figure 4. A) Viability of human fibroblasts exposed to carbonate/percarbonate and B) borate/perborate samples (mean ± SD; $N = 3$, $^{**}P < 0.01$; $^{***}P < 0.001$; $^{****}P < 0.0001$).

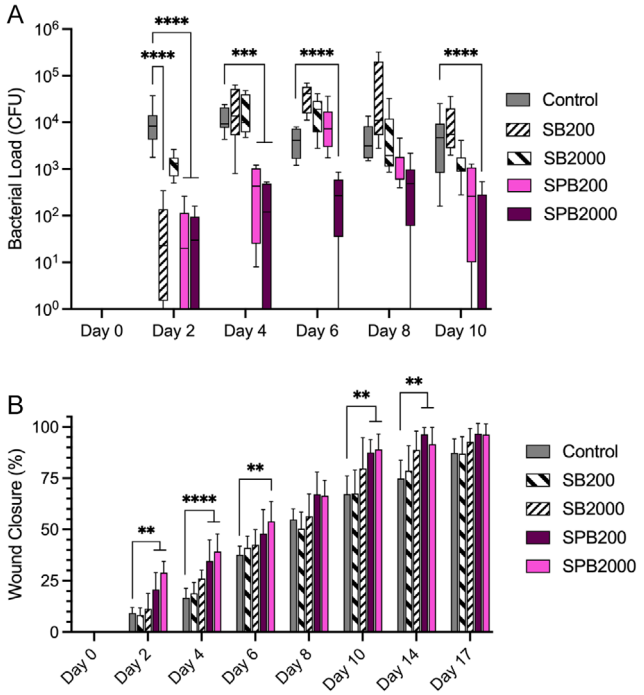

Figure 5. In vivo performance of sodium borate (SB200 and SB2000) and SPB (SPB200 and SPB2000) loaded films. A) Bacterial load quantification in an ischemic rat wound model (interquartile interval, median ± maximum/minimum; $N = 8$ for each group). B) Quantification of wound closure in an untreated ischemic wound (control) and treated ischemic wounds (mean ± SD; $N = 8$, $^{**}P < 0.01$; $^{***}P < 0.001$, $^{****}P < 0.0001$).

had bacterial levels under the threshold of detection on day 0. At subsequent postoperative time points bacterial load increased by $\approx 10^4$–10^5 in the untreated and borate film treated groups except at day 2 (Figure 5A). Perborate films, however, reduced bacterial load by several log scales to 10^1–10^3. By day 6, SPB200 no longer reduced bacterial load relative to controls, but SPB2000 sustained a significant effect until day 8. At day 10, SPB200- and SPB2000-treated groups had re-established lower bacterial counts compared to control.

The effect of films loaded with either borate or perborate on ischemic wound closure was evaluated in vivo in the same ischemic rat wound model. Wound size was measured at post operative days 0, 2, 4, 6, 8, 10, 14, and 17 ($N = 8$ for all conditions at all time points). Figure S2, Supporting Information shows representative photographs of the wounds at various time points from days 0 to 17. At postoperative day 2, the mean closure of SPB-2000 treated wounds was 28.9% closed, compared to 9.3% for untreated wounds ($P < 0.0001$). At the same time point, mean closure of SPB200 treated wounds was 20.8%, albeit with less significance ($P < 0.01$). SPB2000 and 200 treatments maintained improvements over control wounds over the course of the experiment, closing at day 10 by as much as control wounds had reached by day 17 (Figure 5B). At day 8, P values between the control and SPB200/SPB2000 were $P = 0.027$ and $P = 0.039$ respectively. At day 17, significance values between the control and SPB200/SPB2000 were $P = 0.024$ and $P = 0.032$ respectively.

Interestingly, SB2000 treated groups maintained a greater mean wound closure relative to control wounds though differences were only mildly significant on day 4 and 14 ($P < 0.05$). SB200-treated wound closure was not different from control at any time point. Wound healing results for each treatment and time point with corresponding confidence intervals are shown in Table S1, Supporting Information, and SPB 2000 had 95% confidence interval ranges that did not overlap with controls at any time point observed.

Gross examination of H&E-stained histology samples from control, SPB2000, and SB2000 treated animals at postoperative day 17 demonstrated varying degrees of tissue regeneration that correlated with wound closure results. Control wounds had no or minimal re-epithelialization of wounded tissue (**Figure 6**A,B). In contrast, both SPB2000 and SB2000-treated animals exhibited significant re-epithelialization across most of the wounded surface (Figure 6C–F).

3. Discussion

Our previous work demonstrated that the incorporation of calcium peroxides did not greatly deteriorate the physicochemical properties of a PCL film system (Figure S1, Supporting Information).[13] Scanning electron microscopy of these films made with a variety of solid peroxides did not show appreciable material aggregation.[13] PCL is a well-characterized synthetic, biodegradable, semicrystalline polymer that is commonplace in biomedical applications for drug delivery systems.[25,26] It is

© 2025 The Author(s). Advanced NanoBiomed Research published by Wiley-VCH GmbH

26999307, 2025, 8, Downloaded from https://advanced.onlinelibrary.wiley.com/doi/10.1002/anbr.202500045 by Polytechnique Montreal, Wiley Online Library on [09/03/2026]. See the Terms and Conditions (https://onlinelibrary.wiley.com/terms-and-conditions) on Wiley Online Library for rules of use; OA articles are governed by the applicable Creative Commons License

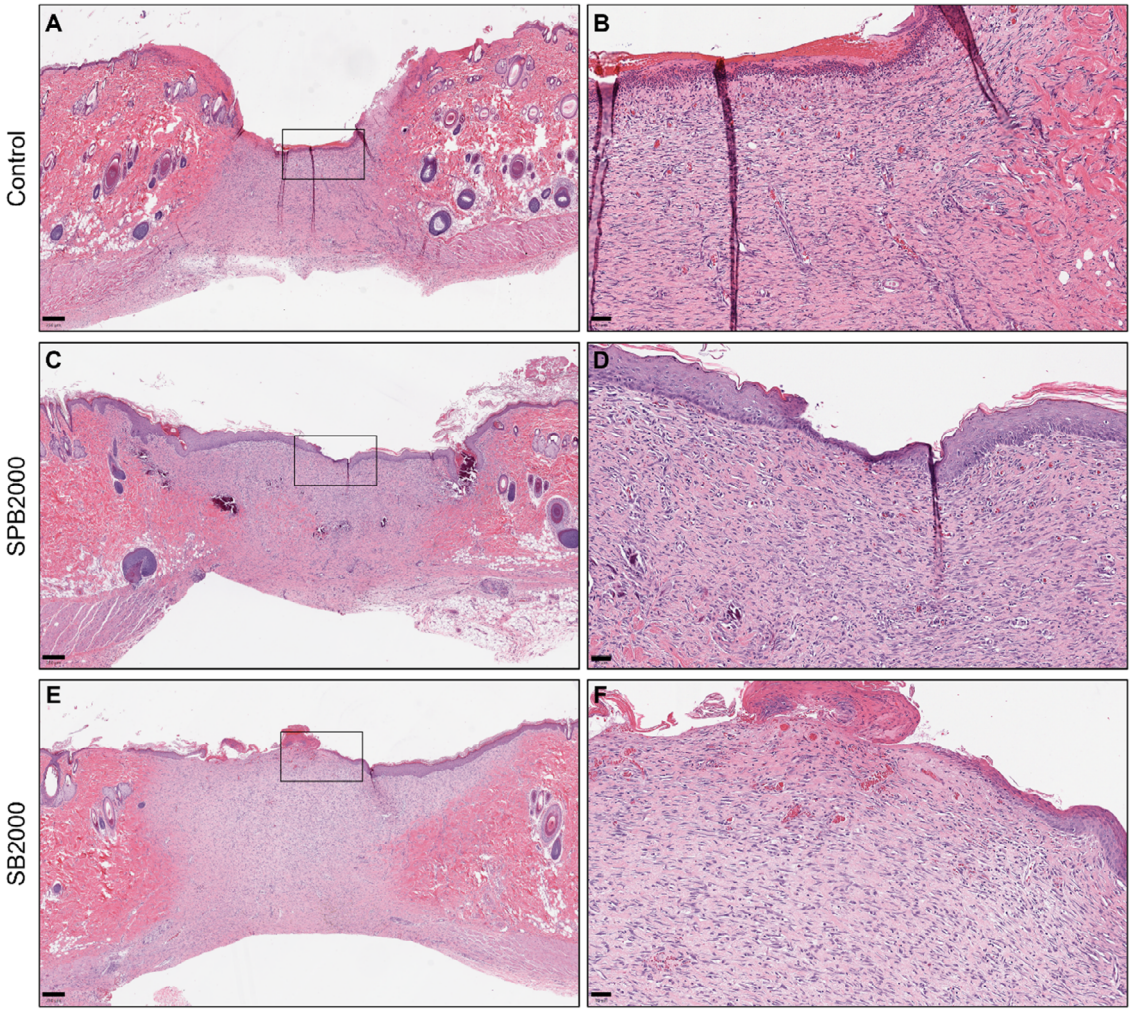

Figure 6. H&E staining of A,B) untreated ischemic, C,D) SPB-treated ischemic, and E,F) sodium borate-treated ischemic wounds. Scale bars on panels A, C, and E: 250 µm; scale bars on panels B, D, and F: 50 µm.

biocompatible, chemically and thermally stable, has a very slow degradation profile, and is tissue compatible.[27] Integration of SPC and SPB increased Young's modulus slightly only at high loading levels (Figure S1A, Supporting Information). All the films were 2–3 times stiffer in comparison to physiological skin (≈140 MPa). For context, commonly used commercial dry wound dressings are <40 MPa, while electrospun PCL dressings are in the range of 5–20 MPa.[28,29] However, these findings align with values reported in the literature for similar PCL composites.[30]

The controlled release profiles of oxygen and hydrogen peroxide from the SPC- and SPB-loaded PCL films are a critical element in determining both antimicrobial efficacy and cellular cytotoxicity. Only at the loading levels of our 2000 mg group did films release appreciable amounts of oxygen (Figure 2A,B), with SPB2000 elevating oxygen levels to maximal values of 571 µM compared to ≈300 µM for SPC2000. Similarly, hydrogen peroxide release in perborate films was roughly triple that of percarbonate films. The molecular weight of SPC is 50% higher than that of SPB (157.01 g mol^{-1} vs. 99.81 g mol^{-1}), meaning it contained roughly 30% less peroxide given a standardized mass; this likely contributed to differences in release assays between equal levels of SPC and SPB. While hydrogen peroxide was already detectable in SPB20, none was measured in SPC20. pH measurements showed that only films in the 2000 mg group approached saturations and in 1.5 mL of water the pH was raised to ≈9.75 and ≈9.25 for SPC and SPB2000 respectively, compared with reported values of 10.5–10.1.[31,32]

Both SPC and SPB films in lower loading level groups did not raise pH out of the pH 7–8 range. However, at the lowest loading level, the SC film did elevate pH to pH 9 and SC 200 and 2000 both raised pH to ≈10, for sodium borate pH elevation was less pronounced such that SB200 and SB2000 raised pH to ≈8.8 and ≈8.9. Comparatively, we treated in vivo wounds with a larger film that contained ≈100 mg of perborate/sample. The 1.5 mL of water used for in vitro pH measurements is likely greater than the volume of fluid found in the wounds used for this study (particularly after the first two postoperative days when wounds are no longer bleeding), suggesting that in vivo pH values would be similar or higher than those measured in vitro.

© 2025 The Author(s). Advanced NanoBiomed Research published by Wiley-VCH GmbH

26999307, 2025, 8, Downloaded from https://advanced.onlinelibrary.wiley.com/doi/10.1002/anbr.202500045 by Polytechnique Montreal, Wiley Online Library on [09/03/2026]. See the Terms and Conditions (https://onlinelibrary.wiley.com/terms-and-conditions) on Wiley Online Library for rules of use; OA articles are governed by the applicable Creative Commons License

SPB has approximately double the solubility of SPC (2.15 g 100 mL^{-1} vs. 1.40 g 100 mL^{-1}), possibly explaining the greater initial H_2O_2 and oxygen release as compared to SPC (Figure 2A–D). It has been reported that the chemical structure of SPB can stabilize generated H_2O_2 molecules, helping to sustain concentration over time since it was observed that hydrogen peroxide decomposed in SPC tests (Figure 2C,D).[33] Conversely, carbonate is known to play a role in the decomposition of H_2O_2, and this may also have been a factor on the apparent decomposition of H_2O_2 observed.[34] Although H_2O_2 concentrations are well known to damage bacterial cell walls, disrupt cellular processes, and inhibit growth, the pH spike associated with highly loaded films can also create an antimicrobial environment.[8,9,35] The modulation of wound pH to promote healing has been a target of several new bioactive dressings.[36–38] A recent systematic review suggested that lowering wound pH improved healing profiles.[39] A report by Siquiera et al. has suggested that alkalinization of the wound microenvironment is key for antibacterial efficacy.[40] Acute wounds are understood to have a more alkaline profile, whereas chronic wounds are more acidic.[41,42] Importantly, pH and O_2 concentration modulation via bioactive dressings is reported to mediate improved re-epithelialization.[43] Both SPB and SPC200 films could increase the wound's pH, potentially exerting a combined antimicrobial effect in the context of local H_2O_2 delivery.

In vitro, borates and carbonates were relatively ineffective against gram-positive (*S. Aureus*) and gram-negative (*P. aeruginosa*) bacterium, with the highest loading levels having slightly greater effect (Figure 3A–D). Perborate and percarbonate films, however, had considerable toxicity against the test bacterial strains. Even the lowest loading levels (SPB and SPC20) were equally or more effective than the highest loading level of corresponding nonperoxide carbonates or borates. Perborate appeared the most potent, with SPB 200 and SPB2000 being essentially equivalent after 2 and 3 days (Figure 3B,D). These data suggest that pH alone was less of a factor than hydrogen peroxide release in antibacterial activity. Biofilm is known to be an important factor in bacterial survival in hostile environments, providing up to 1000 times more antibiotic resistance than that found in planktonic bacteria.[44,45] Previous work has shown that consistent application of high (0.02%, or 5.9 mM) hydrogen peroxide levels is effective in controlling biofilm formation.[46] Our results demonstrated that only the SBP 2000 mg group (H_2O_2 levels ≈600 μM) was effective at limiting biofilm formation, indicating that hydrogen peroxide levels generated by SPC (≈200 μM) were insufficient to prevent biofilm formation (Figure 3E,F). The cytotoxicity of sodium carbonate films against mammalian fibroblast cells was greater than for sodium borates (Figure 4A,B). SPB films were more cytotoxic than their borate counterparts, but only SPB/SPC2000 films were appreciably cytotoxic in vitro. However SC films were more cytotoxic than SB films suggesting pH was the key cause of toxicity.

Given the superior antibacterial action of the perborate films and that only perborate films appreciably inhibited biofilm formation in vitro, we sought to compare the effect of sodium borate (SB) and perborate (SPB) 200 and 2000 films on bacterial count and wound closure in vivo in an ischemic wound model. These films then differed principally in that perborate films released oxygen and hydrogen peroxide; otherwise, the pH and composition of the films was identical. Bacterial load in untreated wounds increased by day 2 (Figure 5A) and then stayed relatively constant until day 10, whereafter the wound was so small and healed (dry) that bacterial counts could not be reliably and meaningfully measured. Only the perborate films reduced bacterial load: SPB 200 did so until day 4 with reduced effect thereafter, and SPB2000 reduced mean values significantly until day 10 apart from postoperative day 8.

It was clear that perborate films could accelerate ischemic healing by approximately a week compared with untreated controls (Figure 5B). We did not determine whether oxygen release was a factor, but certainly the antibacterial action of hydrogen peroxide seemed to be important. Both perborate-loaded materials (200 and 2000 mg) were highly alkaline. The potential contribution of alkalinity to wound healing cannot be discounted since SB2000, which was equally alkaline, also (but to a lesser extent) accelerated early wound closure (Figure 5B). Indeed, when perborate films are compared to borate films rather than untreated controls, the peroxide-based treatments did not result in significantly greater wound closure. Another possible contributory factor to improved wound healing in borate-treated groups compared to untreated controls could be a stimulatory effect of the borate ion itself.[47,48]

Regarding in vitro–in vivo correlation, there were clear discrepancies particularly between mammalian cell cytotoxicity (Figure 4) and the lack of any observed tissue injury (Figure 5 and 6). Cytotoxicity is usually determined in static culture and is appropriate for determining the short-term effects of a fixed concentration of a suspected toxin at levels that might be encountered systemically but would seem of limited value in determining in vivo tissue reactions towards compounds expected to be unstable or reactive in vivo.

There are two perceived issues with inorganic peroxides that many research groups, including ours, have tried to overcome. Firstly, they can be caustic; peroxides are usually impure due to incomplete reaction during manufacturing and contain oxides, which react to form hydroxides and carbonates during storage. The aqueous decomposition product of peroxide is hydroxide. The main approaches to this issue are to use peroxides sparingly or to add acidic salts to create a more neutral mixture. Secondly, peroxides release hydrogen peroxide at levels that may be cytotoxic. The older literature is now informing more recent studies that these assumptions surrounding the 'issues' of inorganic peroxide may at times be incorrect. For example, calcium oxide and hydroxide have been used without pH modification to successfully heal bone, burns, and skin wounds.[49–52] Pastes with pH > 12 were implanted in bone without apparent adverse effects and indeed mineralized tissue was observed around them.[52] Physiological fluid is essentially carbonate-buffered saline with a small amount of phosphate, and so depending on the fluid exchange rate, hydroxide ion release rate, etc., it is conceivable that pH would approach neutrality at the biomaterial surface interface relatively quickly. In addition, blood would be expected to spontaneously clot in contact with alkaline materials and this would further protect the host from caustic burns.[53] Similarly for peroxides, that are to some extent unstable in aqueous conditions, we have shown that the composition of culture media affects hydrogen peroxide stability.[23] In vivo, tissues contain many endogenous peroxidases, such as

© 2025 The Author(s). Advanced NanoBiomed Research published by Wiley-VCH GmbH

26999307, 2025, 8, Downloaded from https://advanced.onlinelibrary.wiley.com/doi/10.1002/anbr.202500045 by Polytechnique Montreal, Wiley Online Library on [09/03/2026]. See the Terms and Conditions (https://onlinelibrary.wiley.com/terms-and-conditions) on Wiley Online Library for rules of use; OA articles are governed by the applicable Creative Commons License

myeloperoxidase, glutathione peroxidases, and catalase and compounds with pseudo-peroxidase action such as hemoglobin such that levels may be expected to vary greatly between in vitro and in vivo conditions.[54–57]

Our findings suggest that lowering wound bacterial load may have been a factor in the observed acceleration of wound closure, at least at early time points, but SPB 200 seemed ineffective in reducing bacterial load after day 4 and yet maintained accelerated wound closure rates comparable to the more antibacterial SPB2000 treatment.

Our work indicates that at the same loading level perborates are more effective antibacterial agents and can accelerate wound closure more than borates (Figure 5 and 6). This may be of benefit in reducing exposure to borates, around which there remain population level safety concerns.[18,19]

Limitations of our work that will be explored in future studies include our wound model; rat skin heals by primarily by contraction and thus wound closure outcomes are not necessarily generalizable to systems that heal primarily by re-epithelialization, as is the case in humans.[58,59] Further, we applied the test materials every two days and so could not determine if a specific stage of healing was affected. The wounds in our study were not sterile postoperatively and did contain significant bacteria; however, there were no clinical signs of infection. Studies with deliberately infected wounds may accentuate differences between materials; however, biofilm inhibition does not infer biofilm disruption which we did not evaluate. Finally, the role of oxygen produced by our materials, if any, was not determined; however, as hydrogen peroxide inevitably generates oxygen in the presence of the many compounds present in wounds capable of decomposing it, and wounds are exposed to the atmosphere which is itself ≈20% oxygen, it would seem difficult and clinically irrelevant to perform experiments that eliminate oxygen at the wound surface.[54–57]

4. Conclusion

Combining perborate and percarbonate compounds into PCL films generated biocompatible polymers with significant antimicrobial function in vitro and in vivo. Wound treatment with an oxygen and hydrogen peroxide-eluting SPB patch at two loading levels (1.5% weight and 13% weight) was found to significantly accelerate ischemic wound healing. In vitro evaluation of biocompatibility with HDFs was not predictive of in vivo tissue response, but bacterial cytotoxicity measured in vitro broadly reflected in vivo results.

5. Experimental Section

Reagents: Sodium percarbonate $2Na_2CO_3{\cdot}3H_2O_2$ (SPC) (371432), sodium carbonate Na_2CO_3 (SC) (223 530) PCL (440744), hydrogen peroxide solution H_2O_2 (30%) (1.07298), sodium bicarbonate $CHNaO_3$ (S5761), Iron (II, III) oxide (637106), chloroform (≥ 99% CH_3Cl_3C), crystal violet (CV) (V5265), and acetic acid (33209) were purchased from Sigma-Aldrich. Calcium dihydrogen phosphate monohydrate $Ca(H_2PO_4)$ (AB119788) was obtained from abcr GmbH. Sodium perborate $NaBO_3{\cdot}H_2O_2$ (SPB) (386410250), sodium borate $NaBO_3$ (SB) (2022010610), and phosphate-buffered saline (PBS) were also obtained.

Preparation of Composite PCL Films: The formulation and manufacturing method have been developed and detailed in previous studies (Figure 1).[13,24,60] Sample toxicity was limited by catalyzing H_2O_2 releases with iron oxide and sodium bicarbonate. Calcium dihydrogen phosphate monohydrate was added to compensate for the acidic pH. PCL was chosen for its hydrophobic properties and biocompatibility.

In this study, two experimental groups were developed: SPC and SPB. Three loading levels were explored for each sodium-based compound: (1) 20 mg, (2) 200 mg, and (3) 2000 mg. Each formulation was prepared with a mixture of 2000 mg of iron (II, III) oxide acting as a catalyst for peroxide decomposition, 500 mg of sodium bicarbonate serving as a primary buffer against large pH fluctuations, and 400 mg calcium dihydrogen phosphate monohydrate as a secondary buffer (**Table 1**). In vitro and in vivo experiments in this study by necessity had different patch sizes, although the relative % w/w of active ingredients remained the same between experiments, such that carbonate/percarbonate and borate/perborate levels increased from 0.15%, 1.5% and 13%.

All materials were passed through a 74 µm sieve (ASTM 200 mesh, Gilson company) before immersion into a 100 mL solution of 10% PCL dissolved in chloroform. The mixtures were magnetically stirred for 4 h and poured into a 190 × 100 mm Pyrex crystallizer (PYREX, No. 3140) and then left to dry for 24 h under a safety hood (Figure 1). Control films were identical to experimental groups, but contained either 1) no peroxide

Table 1. Weight (mg) of the components used to form samples used for tests in this study.

	CNa_2O_3	$Na_2H_3CO_6$	BNa_3O_3	NaH_2BO_4	Fe_3O_4	$CHNaO_3$	$Ca(H_2PO_4)_2$	PCL
Control	0	0	0	0	2000	500	400	10 000
SC20	20	0	0	0	2000	500	400	10 000
SC200	200	0	0	0	2000	500	400	10 000
SC2000	2000	0	0	0	2000	500	400	10 000
SPC20	0	20	0	0	2000	500	400	10 000
SPC200	0	200	0	0	2000	500	400	10 000
SPC2000	0	2000	0	0	2000	500	400	10 000
SB20	0	0	20	0	2000	500	400	10 000
SB200	0	0	200	0	2000	500	400	10 000
SB2000	0	0	2000	0	2000	500	400	10 000
SPB20	0	0	0	20	2000	500	400	10 000
SPB200	0	0	0	200	2000	500	400	10 000
SPB2000	0	0	0	2000	2000	500	400	10 000

© 2025 The Author(s). Advanced NanoBiomed Research published by Wiley-VCH GmbH

26999307, 2025, 8, Downloaded from https://advanced.onlinelibrary.wiley.com/doi/10.1002/anbr.202500045 by Polytechnique Montreal, Wiley Online Library on [09/03/2026]. See the Terms and Conditions (https://onlinelibrary.wiley.com/terms-and-conditions) on Wiley Online Library for rules of use; OA articles are governed by the applicable Creative Commons License

with SC or SB substitution at the same loading level or 2) no peroxide without substitution (control). In vitro assays used circular films 6 mm in diameter, while in vivo experiments used 4×3 cm rectangular patches.

Physicochemical Characterization: To explore the behavior of samples in aqueous media, the swelling index (S.I) was measured after samples had been deposited in vials filled with 10 mL milliQ water for 24 h, 48 h and 72 h. The samples were previously dried for 2 h at 50 °C; then, the mass was measured before testing and at each time point by wiping with microfiber paper to calculate the S.I. according to Equation (1).

$$\text{S.I}(\%) = \frac{W_f - W_i}{W_i} \tag{1}$$

where W_i and W_f are the initial and final weights respectively.

Tensile tests (Instron, 3365) were carried out on 10 × 40 mm pieces to assess Young's modulus and tensile stress at yield. Pneumatic grippers were used to hold the sample under a load of 500 N with a speed of 5 mm min^{-1} and an active length of 25 mm, up to a deformation of 10%. The material was tested dry. The Young's modulus was calculated from sample dimensions and force/extension data.

Quantifying Release: To quantify their H_2O_2 degradation rates, samples were placed in 1.5 mL PBS in microcentrifuge tubes, and after 1, 2, 3, 4, 24, and 48 h, 5 µL of these solutions were added to 150 µL of quantitative peroxide reagents (ThermoFisher, 23280) in 96-well black microplate wells. Aluminum foil was used to cover the plate, and after 15 min, absorbance measurements were taken at 595 nm. Absorbance results were interpreted using an 8-point calibration performed previously by diluting a 30% H_2O_2 solution with PBS between 0 and 500 µM. On the other hand, at each time point, oxygen release measurements were carried out, in same microcentrifuge tubes, using a two-point (0% O_2 and 20.9% O_2) calibrated probe (FOSPOR-AL300) connected to a sensor (NEOFOX-GT, Oceaninsight).

Cytotoxicity and Antioxidant Assay on Human Skin Fibroblasts: HDF extraction, expansion, and usage received Institutional Review Board (IRB) approval by the MUHC Ethics Research Board (approval #MP-37-2020-5995). HDF cells were used between passages 5 and 8 and subcultured after reaching 75% confluency. HDF cells were grown in DMEM media (Gibco) supplemented with 5% fetal bovine serum (Gibco) and 1% PenStrep (Gibco).

Cytotoxicity was assessed using Alamar Blue (ThermoFisher). HDF cells were directly plated in a 48-well plate (ThermoFisher) at a cell density of 3 × 105 in 800 µl of media. One 6 mm disc of material was added to each well. At 24, 48, and 72 h postseeding, culture medium was aspirated and each well containing cells was rinsed with PBS. In accordance with the manufacturer's instructions (ThermoFisher 45), a 10% v/v Alamar blue in fresh medium solution was directly added to each well containing both cells and samples and incubated for 1 h. Following the incubation period, the solution from each well was transferred to a 96-well black UV F-bottom plate. Top and bottom fluorescent readings were measured at emission/excitation wavelengths of 560/590 nm (ThermoFisher Varioskan Lux). The resulting readings were averaged for triplicate samples in each condition and divided by the control sample values to obtain relative viability.

Plate Count Assay: *S. aureus* (ATCC 6538) and *P. aeruginosa* (ATCC 15442) (Cedarlane Laboratories, ON, Canada) were stored at −80 °C until required. To prepare stock cultures, 5 µL of thawed bacteria was inoculated in 5 mL of LB (Luria-Bertani) broth and incubated at 200 rpm, 37 °C for 18 h. The initial concentrations were estimated to be 3×10^{10} and 9×10^{9} colony-forming units (CFU)/mL for *S. aureus* and *P. aeruginosa* respectively. Then, the bacteria strain stock cultures were diluted with nutrient broth (NB 1/500) to achieve the final concentrations of 10^5 CFU/mL. Nutrient broth was made using ISO 22196:2011 by dissolving 3.0 g of meat extract, 10.0 g of peptone, and 5.0 g of sodium chloride in 1000 mL of distilled or deionized water. The obtained solution was diluted with Milli-Q water to a 500-fold volume and adjusted pH between 6.8 and 7.2. The antibacterial efficacy of the resulting samples was examined through the suspension method. In this respect, SPB, SPC films were cut as disks with a size diameter of 6 mm and suspended into the 5 mL diluted bacteria species. The samples were incubated at 37 °C, 200 rpm and at varied incubation times, 24 h, 48 h, and 72 h. Control samples were considered under similar conditions, excluding samples with an antibacterial agent. At the end of the incubation period, 100 µL of aliquots were taken to prepare four serial dilutions with a dilution factor of ten in the saline buffer. Then, the viable bacterial counts were enumerated by spreading 100 µL of diluted aliquots on to the agar Petri dishes incubated overnight at 37 °C. All experiments were repeated in triplicate. Viable bacteria concentration was calculated considering all dilutions made according to Equation (2)

$$\text{Concentration}\,(\text{cfu. ml}^{-1}) = \frac{n \times d}{V} \tag{2}$$

where n is the number of colonies (average of 3 replicates), d the dilution factor, and V the volume of culture plate in mL ($V = 100$ µL). A solution without samples was used as a basis for comparison referred to as the blank.

Biofilm Assay: CV solution 1% and acetic acid were diluted to 0.1% and to 33%, respectively, with milli-Q water. *S. aureus* and *P. aeruginosa* bacterial strains were also used to conduct a biofilm formation assay. A bacterial stock solution was again prepared by inoculating 10 µL of dethawed bacteria in 5 mL LB broth and incubated at 200 rpm, 37 °C for 17–18 h. The stock solution was diluted with LB broth to obtain a 105 CFU/mL bacterial solution. One milliliter of this bacterial solution was incubated with triplicate samples of each condition (SPB, SPC in triplicates) in a 48-well plate, with shaking at 37 °C, for 72 h. Control material to account for the stain absorption was also added to LB in triplicate.

The biofilm formation was then assessed by CV staining: CV stains the biofilm and is released in acetic acid, which allows the quantification of biofilm by an absorbance measurement. The excess bacterial solution in the wells was discarded by careful pipetting, in order not to disturb the biofilm at the surface of the samples. The samples were carefully transferred to a clean well prior to drying for 30 min at 50 °C in an incubator, to dry the biofilm. One hundred fifty microliters of 0.1% CV stain was added to each well and left to incubate for 15 min at room temperature. The wells were then rinsed well with 500 µL milli-Q water at a time until the rinsing solution is clear, to remove the excess CV not staining for biofilm. The samples were left to dry at room temperature before adding 350 µL of 33% acetic acid and incubating for another 15 min, with occasional gentle manual shaking. One hundred microliters of triplicates was pipetted from each well into a 96-well plate, along with 100 µL 33% acetic acid for background. The absorbance at 570 nm was read with a microplate reader (Tecan, Infinite F500). The absorbance of the control sample without bacteria and the background were subtracted from the absorbance of the experimental conditions prior to analysis.

In vivo Ischemic Wound Healing: Surgical Methods: Ethical approval for this work was obtained from the Research Institute of the McGill University Health Center (MUHC-8075) which followed ARRIVE (Animal Research: Reporting of In Vivo Experiments) guidelines. Ten Wistar rats (Charles River Laboratories, USA), 12–14 weeks old and weighing 375–425 g, were allowed to acclimatize for 7 days prior to intervention. The surgical intervention described below has been shown to replicate ischemic wounds and thus was used as a model for evaluating the antibacterial properties of the buffered peroxide composite material. Each animal received carprofen (10 mg kg^{-1}) and slow release buprenorphine (1 mg kg^{-1}) 30 min prior to surgery. Induction and maintenance of anesthesia was accomplished using 2–3% isoflurane. The dorsum of the animal was shaved and disinfected with chlorhexidine wipes, following which a 8 × 4 cm flap was outlined on the on the back with a surgical marker; the spine served as the midline marker for the flap. Five wounds were created on the dorsum using a 8 mm McKesson (#222870) biopsy punch. Four of the wounds were placed within the flap (i.e., ischemic region), and one was placed laterally to the flap on the animal's flank (nonischemic control wound). Full depth lateral incisions were made to elevate the bipedicled flap. The incisions received topical lidocaine and were subsequently closed with simple interrupted sutures using Ethicon polypropylene suture blue monofilament.

A prior knowledge of mean and standard deviation of wound closure and pilot data was used to confirm that $N = 4$ per group was sufficient to

© 2025 The Author(s). Advanced NanoBiomed Research published by Wiley-VCH GmbH

26999307, 2025, 8, Downloaded from https://advanced.onlinelibrary.wiley.com/doi/10.1002/anbr.202500045 by Polytechnique Montreal, Wiley Online Library on [09/03/2026]. See the Terms and Conditions (https://onlinelibrary.wiley.com/terms-and-conditions) on Wiley Online Library for rules of use; OA articles are governed by the applicable Creative Commons License

detect differences with an alpha of 0.01 and a power of 80%, using an online tool, https://clincalc.com/stats/samplesize.aspx. For each rat, the animal received either the SPB 200 mg or 2000 mg polymer patch, a nonoxygenating sodium borate 200 mg or 2000 mg patch, or no treatment (1 patch covered 4 defects/animal, 2 animals per group). The patches were replaced for a new film of the same type at every bandage change (days 2, 4, 6, 8, and 10). The nonischemic control wound on the animals' flank did not receive any treatment. The patches were washed with sterile saline and then applied to the ischemic wounds. The surgical site was then dressed with a 3M Tegaderm bandage. Animals received carprofen (10 mg kg^{-1}) every 24 h 3 days postoperatively. Animals were allowed free access to food and water and housed in a 12-h day/night cycle. All animals were sacrificed via CO_2 asphyxiation following confirmed sedation by 4% isoflurane.

In Vivo Ischemic Wound Healing: Dressing Preparation and Change: Prior to dressing the wound in both animal models, patches were washed with saline. The wounds were cleaned were cleaned with sterile saline and the dressing was applied directly to the wounds and covered with a Tegaderm dressing. Dressings/patches were replaced every 2 days until postoperative day 10, after which they were changed one more time at postoperative day 14.

In Vivo Ischemic Wound Healing: Wound Size Measurement: At each dressing change, pictures of the ear were taken using standard lighting, zoom and distance with a scale included in the image. Dimensions of the wounds were calculated from the photos for each time point using ImageJ software.

In Vivo Ischemic Wound Healing: Bacterial Culture: Bacterial cultures were collected every two days at the time of dressing change until postoperative day 10 to evaluate the antibacterial profile of the polymeric biomaterials. The skin around each wound was cleaned with saline, and sterile swabs were used to collect samples from the wound surface. Once the wound had begun to scab over in the later postoperative stages, scabs were debrided, and swabs were collected from the underlying tissue (i.e., the wound bed). Following collection, swabs were inserted into 1 mL of Luria–Bertani media (LB) in a 2 mL Eppendorf tube. Samples were subsequently diluted 10 times in 900 µL LB media and spread-plated on LB agar. After a 16 h incubation period at 37 °C, the colonies were enumerated to ascertain the CFU per mL.

CFU was determined using the formula

$$CFU = number\ of\ colonies \div quantity\ plated \times dilution\ factor \quad (3)$$

Statistical Analysis and Reproducibility: All in vitro results ($N = 3$–9) and in vivo wound healing results ($N = 8$) were expressed as mean ± standard deviation. In vivo bacterial quantification was represented using a box-and-whisker plot. Statistics were performed on logarithms of measured values for data represented with a logarithmic scale. Differences between groups and time points was assessed using one-way analysis of variance and a Tukey post hoc test using a calculator tool https://statpages.info/anova1sm.html. Data difference statistics and figure generation was performed on GraphPad Prism version 10.4.1 for Windows (GraphPad Software, Boston, Massachusetts USA). As preclinical data are inherently variable, statistical significance was determined with a threshold of $P < 0.01$, which correlated with findings that were likely to be clinically significant, with robust differentiation between treatment effects. 95% confidence intervals were calculated using Microsoft Excel (Table S1, Supporting Information). Image analyses values were repeated by a second operator blinded to sample identification and were found to be within 5% or less of values obtained by the original investigator.

Supporting Information

Supporting Information is available from the Wiley Online Library or from the author.

Acknowledgements

D.J. and A.W. contributed equally to this work and should be considered cofirst authors. Professors G.M. and J.B. contributed equally to this work. We acknowledge the support of NSERC for the provision of Discovery Grants (J.B., G.M.) that supported this work.

Conflict of Interest

The authors declare no conflict of interest.

Data Availability Statement

The data that support the findings of this study are available from the corresponding author upon reasonable request.

Keywords

antibacterial, biomaterials, borate, carbonate, peroxide, skin, wound healing

Received: February 20, 2025
Revised: April 10, 2025
Published online: June 26, 2025

[1] C. J. L. Murray, K. S. Ikuta, F. Sharara, L. Swetschinski, G. Robles Aguilar, A. Gray, C. Han, C. Bisignano, P. Rao, E. Wool, S. C. Johnson, A. J. Browne, M. G. Chipeta, F. Fell, S. Hackett, G. Haines-Woodhouse, B. H. Kashef Hamadani, E. A. P. Kumaran, B. McManigal, S. Achalapong, R. Agarwal, S. Akech, S. Albertson, J. Amuasi, J. Andrews, A. Aravkin, E. Ashley, F.-X. Babin, F. Bailey, S. Baker, et al., *Lancet* **2022**, *399*, 629.
[2] W. C. Reygaert, *AIMS Microbiol.* **2018**, *4*, 482.
[3] C.-H. Wang, Y.-H. Hsieh, Z. M. Powers, C.-Y. Kao, *Int. J. Mol. Sci.* **2020**, *21*, 1061.
[4] A. R. M. Coates, Y. Hu, J. Holt, P. Yeh, *Expert Rev. Anti. Infect. Ther.* **2020**, *18*, 5.
[5] K. Davis, T. Greenstein, R. Viau Colindres, B. B. Aldridge, *Curr. Opin. Microbiol.* **2021**, *64*, 68.
[6] R. J. White, K. Cutting, A. Kingsley, *Ostomy Wound Manage.* **2006**, *52*, 26.
[7] F. Yousefian, R. Hesari, T. Jensen, S. Obagi, A. Rgeai, G. Damiani, C. G. Bunick, A. Grada, *Antibiotics Basel.* **2023**, *12*, 1434.
[8] G. Zhu, Q. Wang, S. Lu, Y. Niu, *Med. Princ. Pract.* **2017**, *26*, 301.
[9] M. V. Urban, T. Rath, C. Radtke, *Wien Med. Wochenschr.* **2019**, *169*, 222.
[10] M. P. Murphy, H. Bayir, V. Belousov, C. J. Chang, K. J. A. Davies, M. J. Davies, T. P. Dick, T. Finkel, H. J. Forman, Y. Janssen-Heininger, D. Gems, V. E. Kagan, B. Kalyanaraman, N.-G. Larsson, G. L. Milne, T. Nyström, H. E. Poulsen, R. Radi, H. Van Remmen, P. T. Schumacker, P. J. Thornalley, S. Toyokuni, C. C. Winterbourn, H. Yin, B. Halliwell, *Nat. Metab.* **2022**, *4*, 651.
[11] H. Van Acker, T. Coenye, *Trends Microbiol.* **2017**, *25*, 456.
[12] B. J. Juven, M. D. Pierson, *J. Food Prot.* **1996**, *59*, 1233.
[13] D. Job, J. Matta, C.-T. Dang, Y. Raphael, J. Vorstenbosch, B. Helli, G. Merle, J. Barralet, *MedComm Biomater. Appl.* **2024**, *3*, e75.
[14] Y.-H. Lai, S. Roy Barman, A. Ganguly, A. Pal, J.-H. Yu, S.-H. Chou, E. W. Huang, Z.-H. Lin, S.-Y. Chen, *Chem. Eng. J.* **2023**, *476*, 146744.
[15] P. Singh, S. M. Andrabi, U. Tariq, S. Gupta, S. Shaikh, A. Kumar, *Chem. Eng. J.* **2023**, *457*, 141359.

 © 2025 The Author(s). Advanced NanoBiomed Research published by Wiley-VCH GmbH

26999307, 2025, 8, Downloaded from https://advanced.onlinelibrary.wiley.com/doi/10.1002/anbr.202500045 by Polytechnique Montreal, Wiley Online Library on [09/03/2026]. See the Terms and Conditions (https://onlinelibrary.wiley.com/terms-and-conditions) on Wiley Online Library for rules of use; OA articles are governed by the applicable Creative Commons License

[16] L. Zhou, S. Guo, Z. Dong, P. Liu, W. Shi, L. Shen, J. Yin, *Mater. Today Adv.* **2024**, *21*, 100458.
[17] Y. Yan, M. Wang, M. Zhao, J. Zhang, Y. Liu, X. Gao, *Adv. Healthcare Mater.* **2023**, *12*, e2301375.
[18] (US) AfTSaDR. Toxicological Profile for Boron. Atlanta (GA): Agency for Toxic Substances and Disease Registry (US) **2010**, Health Effects. https://www.ncbi.nlm.nih.gov/books/NBK599075/.
[19] K. H. Beyer, W. F. Bergfeld, W. O. Berndt, R. K. Boutwell, W. W. Carlton, D. K. Hoffmann, A. L. Schroeter, *J. Am. Coll. Toxicol.* **1983**, *2*, 87.
[20] P. Sofokleous, S. Ali, P. Wilson, A. Buanz, S. Gaisford, D. Mistry, A. Fellows, R. M. Day, *Acta Biomater.* **2017**, *64*, 301.
[21] M. Betz, G. Cerny, *Tenside, Surfactants, Deterg.* **2000**, *37*, 230.
[22] P. Grandjean, *Basic Clin. Pharmacol. Toxicol.* **2016**, *119*, 126.
[23] A. Rastinfard, B. Dalisson, J. Barralet, *Acta Biomater.* **2022**, *145*, 390.
[24] Y. Ouhaddi, B. Dalisson, A. Rastinfard, M. Gilardino, K. Watters, D. Job, P. Azizi-Mehr, G. Merle, A. V. Lasagabaster, J. Barralet, *Biomater. Adv.* **2023**, *153*, 213519.
[25] E. Malikmammadov, T. E. Tanir, A. Kiziltay, V. Hasirci, N. Hasirci, *J. Biomater. Sci. Polym. Ed.* **2018**, *29*, 863.
[26] S. Jiang, Y. Chen, G. Duan, C. Mei, A. Greiner, S. Agarwal, *Polym. Chem.* **2018**, *9*, 2685.
[27] M. J. Mochane, T. S. Motsoeneng, E. R. Sadiku, T. C. Mokhena, J. S. Sefadi, *Appl Sci.* **2019**, *9*, 2205.
[28] M. Minsart, S. Van Vlierberghe, P. Dubruel, A. Mignon, *Burns Trauma.* **2022**, *10*, tkac024.
[29] Y. Wang, X. Wang, D. Zhou, X. Xia, H. Zhou, Y. Wang, H. Ke, *ACS Omega.* **2023**, *8*, 20323.
[30] J. Wei, S. J. Heo, D. H. Kim, S. E. Kim, Y. T. Hyun, J. W. Shin, *J. R. Soc. Interface* **2008**, *5*, 617.
[31] Massachusetts Department of Environmental Protection, Hydrogen Peroxide, Peracetic Acid and Sodium Percarbonate www.mass.gov, (accessed March 2010).
[32] B. John, D. H. Colin, Chapter Six - Catalysis or Convenience? Perborate in Context Ed. R. van Eldik, C. D. Hubbard. *Adv Inorg Chem*, Academic Press **2013**, *65*, pp. 217–310.
[33] M. Grootveld, E. Lynch, G. Page, W. Chan, B. Percival, E. Anagnostaki, V. Mylona, S. Bordin-Aykroyd, K. L. Grootveld, *Dent. J. Basel.* **2020**, *8*, 89.
[34] A. Jawad, Z. Chen, G. Yin, *Chin. J. Catal.* **2016**, *37*, 810.
[35] A. Singh, A. Dubey, *ACS Appl. Bio Mater.* **2018**, *1*, 3.
[36] S. Tyeb, N. Kumar, *Soft Mater.* **2022**, *20*, 379.
[37] J. Koehler, L. Wallmeyer, S. Hedtrich, A. M. Goepferich, F. P. Brandl, *Macromol. Biosci.* **2017**, *17*, 1600369.
[38] S. Jung, S. Chang, N.-E. Kim, Y.-J. Song, J. Kim, *Macromol. Mater. Eng.* **2023**, *308*, 2300141.
[39] R. Derwin, D. Patton, P. Avsar, H. Strapp, Z. Moore, *Int. Wound J.* **2022**, *19*, 1397.
[40] J. F. Siqueira, M. de Uzeda, *J. Endod.* **1998**, *24*, 663.
[41] C. R. Kruse, M. Singh, S. Targosinski, I. Sinha, J. A. Sørensen, E. Eriksson, K. Nuutila, *Wound Repair Regen.* **2017**, *25*, 260.
[42] V. Vivcharenko, A. Przekora, *Appl. Sci.* **2021**, *11*, 4114.
[43] G. Schoukens 5 - Bioactive Dressings to Promote Wound Healing. Ed. S. Rajendran, *Advanced Textiles for Wound Care* (Second Edition) Woodhead Publishing **2019**. pp. 135–167.
[44] J. Olivares, A. Bernardini, G. Garcia-Leon, F. Corona, *Front Microbiol.* **2013**, *4*, 103.
[45] K. Iskandar, J. Murugaiyan, D. Hammoudi Halat, S. E. Hage, V. Chibabhai, S. Adukkadukkam, C. Roques, L. Molinier, P. Salameh, M. Van Dongen, *Antibiotics Basel.* **2022**, *11*, 182.
[46] M. A. Hoogenkamp, D. Mazurel, E. Deutekom-Mulder, J. J. de Soet, *Biofilm* **2023**, *5*, 100132.
[47] L. Hadidi, S. Ge, M. Comeau-Gauthier, J. Ramirez-Garcia Luna, E. J. Harvey, G. Merle, *J. Orthop. Trauma.* **2021**, *35*, e165.
[48] N. Sedighi-Pirsaraei, A. Tamimi, F. Sadeghi Khamaneh, S. Dadras-Jeddi, N. Javaheri, *Front. Bioeng. Biotechnol.* **2024**, *12*, 1475584.
[49] D. F. Mitchell, G. B. Shankwalker, *J. Dent. Res.* **1958**, *37*, 1157.
[50] F. Gong, N. Yang, J. Xu, X. Yang, K. Wei, L. Hou, B. Liu, H. Zhao, Z. Liu, L. Cheng, *Adv. Healthcare Mater.* **2023**, *12*, 2201771.
[51] T. Takayama, M. Ishihara, S. Nakamura, Y. Sato, S. Hiruma, K. Fukuda, K. Murakami, H. Yokoe, *Int. J. Mol. Sci.* **2020**, *21*, 4176.
[52] A. Stavropoulos, C. Geenen, J. R. Nyengaard, T. Karring, A. Sculean, *Clin. Oral. Implants Res.* **2007**, *18*, 761.
[53] C. Chaimoff, D. Creter, M. Djaldetti, *Am. J. Surg.* **1978**, *136*, 257.
[54] R. Ihalin, V. Loimaranta, Tenovuo J. Origin, *Arch. Biochem. Biophys.* **2006**, *445*, 261.
[55] A. I. Alayash, M. T. Wilson, *Front Mol. Biosci.* **2022**, *9*, 910795.
[56] X. G. Lei, *Methods Enzymol.* **2002**, *347*, 213.
[57] H. Sies, *J. Biol. Chem.* **2014**, *289*, 8735.
[58] D. S. Masson-Meyers, T. A. M. Andrade, G. F. Caetano, F. R. Guimaraes, M. N. Leite, S. N. Leite, M. A. C. Frade, *Int. J. Exp. Pathol.* **2020**, *101*, 21.
[59] D. G. Sami, H. H. Heiba, A. Abdellatif, *Wound Med.* **2019**, *24*, 8.
[60] H. Zhang, B. Dalisson, S. Tran, J. Barralet, *Adv Healthcare Mater.* **2018**, *7*, 1701338.

 © 2025 The Author(s). Advanced NanoBiomed Research published by Wiley-VCH GmbH

26999307, 2025, 8, Downloaded from https://advanced.onlinelibrary.wiley.com/doi/10.1002/anbr.202500045 by Polytechnique Montreal, Wiley Online Library on [09/03/2026]. See the Terms and Conditions (https://onlinelibrary.wiley.com/terms-and-conditions) on Wiley Online Library for rules of use; OA articles are governed by the applicable Creative Commons License